Veličković *et al. Plant Methods* (2024) 20:117
https://doi.org/10.1186/s13007-024-01249-5

Plant Methods

METHODOLOGY Open Access

RhizoMAP: a comprehensive, nondestructive, and sensitive platform for metabolic imaging of the rhizosphere

Dušan Veličković[1*], Tanya Winkler[1], Vimal Balasubramanian[1], Thomas Wietsma[1], Christopher R. Anderton[1], Amir H. Ahkami[1] and Kevin Zemaitis[1]

Abstract

Background Elucidating the intricate structural organization and spatial gradients of biomolecular composition within the rhizosphere is critical to understanding important biogeochemical processes, which include the mechanisms of root-microbe interactions for maintaining sustainable plant ecosystem services. While various analytical methods have been developed to assess the spatial heterogeneity within the rhizosphere, a comprehensive view of the fine distribution of metabolites within the root-soil interface has remained a significant challenge. This is primarily due to the difficulty of maintaining the original spatial organization during sample preparation without compromising its molecular content.

Results In this study, we present a novel approach, RhizoMAP, in which the rhizosphere molecules are imprinted on selected polymer membranes and then spatially profiled using matrix-assisted laser desorption/ionization (MALDI) mass spectrometry imaging (MSI). We enhanced the performance of RhizoMAP by combining the use of two thin (< 20 µm) membranes (polyester and polycarbonate) with distinct MALDI sample preparations. This optimization allowed us to gain insight into the distribution of over 500 different molecules within the rhizosphere of poplar (*Populus trichocarpa*) grown in rhizoboxes filled with mycorrhizae soil. These two membranes, coupled with three different sample preparation conditions, enabled us to capture the distribution of a wide variety of molecules that included phytohormones, amino acids, sugars, sugar glycosides, polycarboxylic acids components of the Krebs cycle, fatty acids, short aldehydes and ketones, terpenes, volatile organic compounds, fertilizers from the soil, and others. Their spatial distribution varies greatly, with some following root traces, others showing diffusion from roots, some associated with soil particles, and many having distinct hot spots along the plant root or surrounding soil. Moreover, we showed how RhizoMAP can be used to localize the origin of the molecules and molecular transformation during root growth. Finally, we demonstrated the power of RhizoMAP to capture molecular distributions of key metabolites throughout a 20 cm deep rhizosphere.

Conclusions RhizoMAP is a method that provides nondestructive, untargeted, broad, and sensitive metabolite imaging of root-associated molecules, exudates, and soil organic matter throughout the rhizosphere, as demonstrated in a lab-controlled native soil environment.

*Correspondence:
Dušan Veličković
dusan.velickovic@pnnl.gov

Full list of author information is available at the end of the article

Keywords Rhizosphere, Metabolite imaging, Root exudates, MALDI, Mass spectrometry, Spatial distribution, Imprinting, Rhizobox

Background

The rhizosphere is the region of soil proximal to a plant's root system, where this microenvironment is directly influenced by root secretions, the soil microorganisms, and their related metabolic and biogeochemical processes [1]. The rhizosphere is one of the most dynamic and vibrant terrestrial ecosystems, functioning as a hotspot for plant-soil-microbe interactions that can significantly influence carbon and nutrient cycles at a global scale [1, 2]. Revealing molecular heterogeneities in the rhizosphere is necessary to develop new mechanistic models that can enable our ability to understand the dynamic, spatiotemporal, and microscale processes that affect ecosystem sustainability and crop productivity. Therefore, developing techniques that enable imaging of the rhizosphere and that will provide the microscale spatial context in situ is of great importance [3].

There are numerous approaches that have been recently developed for analyzing chemical and molecular heterogeneity throughout the rhizosphere. For example, a correlative imaging workflow for targeted sampling of roots in three dimensions enabled visualization of ^{13}C enriched zones and Ca^{2+} and Cl^- channel gradients [4], optode systems provided the ability to measure O_2, pH, and CO_2 gradients [5], and zymographic approaches afforded insight into enzymatic activity along the root within the rhizosphere [6, 7]. However, an analytical grand challenge remains in imaging exudates and metabolites within the rhizosphere. Mass spectrometry imaging (MSI) is a ubiquitous method for spatial metabolite profiling of biological samples. However, it remains impractical for direct analysis of the rhizosphere, as it requires *ex-situ* processing, and it is impossible to preserve the in-situ spatial organization of the roots and surrounding rhizosphere without compromising molecular content [8]. Indeed, some efforts have enabled direct imaging of plant metabolites in the rhizosphere, employing MSI to analyze embedded root cross-sections and the surrounding soil [9]. However, using such a cross-sectional approach to assess the gradient of the root exudation along the root or reveal its interaction across the rest of the root network would be tremendously laborious and expensive in practice. Moreover, this destructive approach requires plant harvesting and cryosectioning, so it cannot be applied temporally within the same plant.

To address those challenges, we and others have developed synthetic soil habitats compatible with MSI [10]. These polymer-based microfluidic systems mimic soil physical properties and afford us the ability to visualize amino acid gradients along the roots network, for example [10]. Nevertheless, this approach has several limitations, including the relatively small size of the plants that can be grown within these microhabitats, the inability to perform time-series measurements from the same sample, and they do not mimic soil chemistry, which is an important component of the rhizosphere. As an alternative, we recently developed a workflow based on transferring (i.e., imprinting) the molecules from the rhizosphere onto polyvinylidene fluoride (PVDF) membranes, which are then spatially profiled using matrix-assisted laser desorption/ionization (MALDI)-MSI [11]. While this process was efficient and allowed the visualization of metabolites within the rhizosphere, this approach only provided limited molecular coverage (i.e., the number of molecules and molecular classes measurable). We anticipated that further studies utilizing different membrane materials, MALDI matrices, and MSI conditions would adequately capture the richness of organic molecules within the rhizosphere [11]. Recently, others successfully modified this workflow and utilized desorption electrospray ionization (DESI)-MSI to image PVDF rhizosphere imprints, where they expanded the detectable metabolome to include organic acids [12].

Herein, we developed a platform called RhizoMAP, where we advanced our MALDI-MSI workflow for imprinting the rhizosphere in rhizoboxes filled with soil by optimizing new membrane chemistries in conjunction with several additional sample preparation conditions. Through these efforts, we enabled visualization and insight into the spatial distributions of over 500 molecular species in the poplar (*Populus trichocarpa*) rhizosphere. The molecules detected comprised a wide range of primary metabolites, secondary metabolites, volatile organic compounds, soil fertilizers, and others. Given the localizations of these metabolites within the channels and pores of soil or along the root traces within the rhizosphere, these results provide the most comprehensive map of the metabolic network in the rhizosphere so far.

Methods

RhizoMAP workflow is illustrated in Fig. 1, and each procedure is discussed in detail in the following subsections.

Rhizobox design

The rhizoboxes were designed and built at PNNL. The rhizoboxes are constructed of an acetal resin frame with two 9.5 mm thick removable clear Polycarbonate panels. The inner dimension is 35.6×38.1×2.5 cm (h × w × d), and the inner volume is 3445.2 cm^3. The rhizoboxes can be fitted with support legs that tilt the boxes at a 60

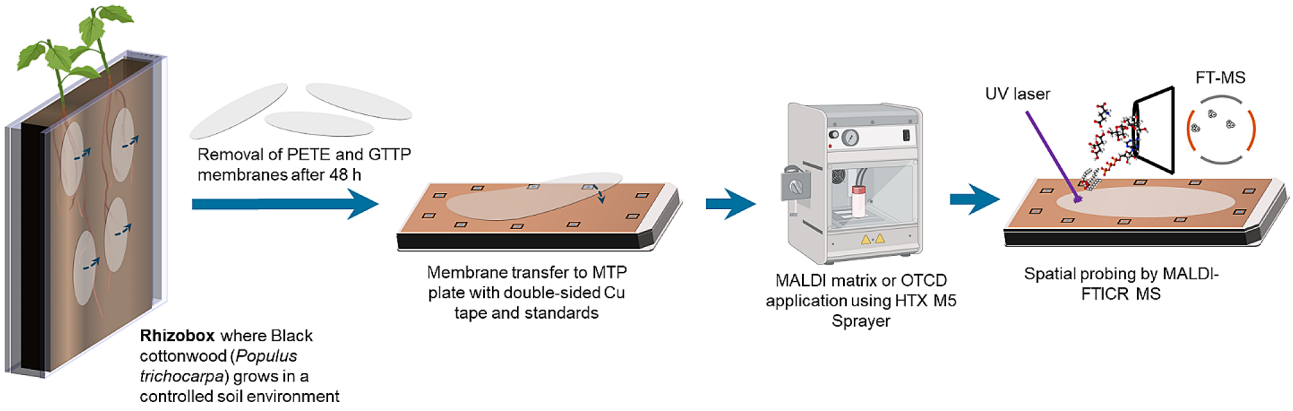

Fig. 1 Overview of the RhizoMAP workflow. Imprinting membranes (PETE and GTTP) are placed on the roots of plants growing in the Rhizobox. After 48 h, membranes are removed and mounted on the MALDI target (MTP) plate using double-sided Cu tape. On-target chemical derivatization (OTCD) and MALDI matrix applications are performed by an automatized spraying device (HTX TM5 Sprayer), and the imprinting membrane is analyzed by MALDI FTICR MS

degree (30 degree from vertical) during the experiment. The rhizobox schematic is provided in the Supplementary document.

Plant growth

Populus trichocarpa cuttings were propagated in Pro-Mix BX with Mycorrhizae growing medium (Pro-Mix, PA, USA). Small stem cuttings with a leaf and node are taken from a lateral stem of a parent plant, and the leaf area is trimmed down to have around 2.5 cm of surface area to reduce transpiration. The cutting was soaked in 1% Zerotol for a few minutes, then the base of the stem is dipped in Rhizopon rooting powder (Rhizopon AA#2, Hortus USA Corp., NY, USA) and inserted into the soil in 10 cm pots. The cuttings were kept in the tray under a humidity dome and misted daily in a growth chamber with a temperature of 24 °C /18°C (day/night), a light intensity of 400 µM/s and a photoperiod of 16 h/8 h (day/night) at 60% humidity. After 3–4 weeks, most cuttings formed roots. Healthy young plants with roots were selected to transplant into the rhizoboxes. The boxes were filled with soil (Pro-Mix, PA, USA), leaving some room for the plants. The plants were positioned with the roots along the side of the box, the box was tilted, and soil was added to fill in the area and complete the planting. The plant was then fertilized with 30 mL of Jacks Pro fertilizer (JR Peters, PA, USA) to help it get established. The plants were watered every other day and fertilized once a week with 30 mL of fertilizer if no testing was being done and were grown under the same growth chamber environmental conditions for 4 weeks. The boxes were positioned at a 60° angle with the planted root side on the bottom so that the roots would grow along the side of the box.

Imprinting and sample collection

Hydrophilic polycarbonate (GTTP04700, 0.22 µm pore size, 17 µm thickness, Merc Millipore, Tulagreen, Ireland) and hydrophilic polyester (PETE; STU1300027, 3.0 µm pore size, 12 µm thickness, Sterlitech, Auburn, WA) membrane filters (47 mm diameter) were used in this study. These membranes were selected due to their small thickness (<20 µm), which makes them compatible with MALDI MS imaging analysis, and their hydrophilic character allows them to extract root exudates. Membranes were placed on the different root zones between the plexiglass and root-soil interface and left in place for 48 h, tightening the plexiglass panel with screws to ensure pressure and constant contact between membranes and root-soil interface (Supplementary Figure S1). Membranes were also placed the same way in a Rhizobox filled only with the PRO-MIX BX mycorrhizae soil (Premier Tech, PA, US) without a plant. After 48 h, membranes were removed from the Rhizoboxes, dried under vacuum, vacuum sealed, and stored at -20 °C until processing for MSI. After membrane harvesting, 1 g of rhizosphere below the membrane was removed for bulk measurements, where organics were extracted using the methanol-water sequential protocol previously developed in our laboratory [13]. We named this fraction bulk rhizosphere extract.

Mass spectrometry imaging and data processing

Imprinted and clean (blank) membranes were mounted on an MTP 384 target (8280784, Bruker Daltonic, Billerica, MA) using double-sided adhesive copper tape (3-6-1182, 3 M, USA). Briefly, using forceps, one edge of the membrane is placed on the adhesive copper tape, and through electrostatic attraction and additional positioning using forceps, the rest of the membrane is adhered to the copper tape, gently laying the membrane onto the surface (Fig. 1). This is done carefully, and to ensure the

entire membrane is fully secured to the plate, the membrane is rolling flat using a clean 20 mL scintillation vial. 5 µL droplets of bulk rhizosphere extract and 1 µL droplets of the abscisic acid standard (1 mg/mL in 50% methanol (MeOH) v/v) were pipetted beside the membranes on the copper tape and let dry. Samples were then sprayed with MALDI matrices using an M5 sprayer (HTX Technologies, Chapel Hill, NC, USA) under three conditions; the nozzle height was adjusted to 52 mm to maintain a 40 mm distance to the sample for direct spraying on MTP 384 targets. N-(1-naphthyl) ethylenediamine dihydrochloride (NEDC; Sigma-Aldrich, St. Louis, MO, USA) was used for negative ion mode experiments. NEDC was prepared at a 7 mg/mL concentration in 70% MeOH (v/v) and sprayed at a 120 µL/min flow rate. The nozzle temperature was set to 70 °C, with eight cycles at 3-mm track spacing with a crisscross pattern. A 0-s drying period was added between cycles, and a linear flow was set to 1,200 mm/min with 10 PSI of nitrogen gas. This resulted in a matrix coverage of ~187 µg/cm^2 for NEDC. For positive mode analysis, two applications were performed: with and without on-target chemical derivatization (OTCD) using 4-(2-((4-bromophenethyl) dimethylammonio)ethoxy)benzenaminium bromide (4-APEBA) [14]. For non-derivatized samples, DHB (2,5-dihydroxybenzoic acid; Sigma-Aldrich, St. Louis, MO, USA) was prepared at a concentration of 40 mg/mL in 70% MeOH and was sprayed at a 50 µL/min flow rate. The nozzle temperature was set to 70 °C, with 12 cycles at 3 mm track spacing with a crisscross pattern. A 2 s drying period was added between cycles, and a linear flow was set to 1,200 mm/min with 10 PSI of nitrogen gas. This resulted in a matrix coverage of ~667 µg/cm2 for DHB. For OTCD, we used our established two-step approach [15] by spraying an aqueous solution of 1-ethyl-3-(3-dimethylaminopropyl)carbodiimide (EDC; Sigma-Aldrich, St. Louis, MO, USA) at 6 mg/mL first with subsequent application of 4-APEBA at 2 mg/mL using an external syringe pump. Spraying parameters were the same for both chemicals: a 25 µL/min flow rate, a nozzle temperature of 37.5 °C, four cycles at 3-mm track spacing with a crisscross pattern, a 2-s drying period, 1,200 mm/min spray head velocity, 10 PSI of nitrogen gas. Immediately after derivatization, DHB was sprayed using the same conditions as for non-derivatized samples.

MALDI-MSI was performed on a 12T solariX FTICR MS equipped with a ParaCell analyzer and a dual ESI/MALDI source, where the MALDI source used a SmartBeam II (355 nm) laser (Bruker Daltonics, Bremen, Germany). For both positive and negative ion modes, acquisitions were acquired with broadband excitation from m/z 98.3 to 1,000, resulting in a detected transient of 0.5593 s—the observed mass resolution was ~110k at m/z 400. FlexImaging (Bruker Daltonics, v.5.0) was used for the imaging experiments, and analyses were performed with a 200 µm step size. FlexImaging sequences were directly imported into SCiLS Lab (Bruker Daltonics, v.2023.a Premium 3D) using automatic magnetic resonance mass spectrometry (MRMS) settings. Ion images were directly processed from the profile data sets within SCiLS Lab, using the root mean square (RMS) normalization, and automated annotation of the centroided data set was completed within METASPACE with a chemical modifier corresponding to the mass shift expected from 4-APEBA derivatization (+$C_{18}H_{22}N_2Br$, +345.0966 Da) if 4-APEBA OTCD was performed. KEGG-v1 was used as a metabolite database for annotations. METASPACE actions tool "Compare with other datasets" was used to select annotations not present in the corresponding clean (blank) membranes.

Results

Hydrophilic polyester track etched (PETE) and hydrophilic polycarbonate (GTTP) membranes were evaluated as imprinting materials for RhizoMAP. Together with three sample preparation conditions (two different MALDI matrices and 4-APEBA OTCD), our method enabled the spatial detection of nearly 500 different molecules in the rhizosphere of poplar plants grown in the Rhizoboxes filled with mycorrhizae soil (Fig. 2). This optimization resulted in a 10-fold improvement compared to our previously published workflow utilizing PVDF membranes, where roughly 40 metabolites were confidently annotated from a similar system [11].

PETE and GTTP membranes ensured stable total ion count during the entire imaging run in negative ionization mode and, even more, showed compatibility with 4-APEBA derivatization—however, the membranes provided quite different molecular profiles of the rhizosphere (Fig. 2). When 4-APEBA was used, of the molecules detected from the rhizosphere, there was only a ~9% (11 out of 121 ions) overlap between PETE and GTTP. GTTP captured slightly more molecules annotated from the bulk extract (Fig. 2B), although the bulk extract generally showed different molecular composition than molecules imprinted on the membranes (70 molecules from the bulk were not captured, and 33 molecules from the bulk were captured on membranes, Fig. 2B). NEDC, as the MALDI matrix, provided a more significant molecular overlap between the two membranes and bulk extracts (Fig. 2C), where 100 different molecules were common for all three conditions, and in total, only 20 out of 194 annotated features were not captured on membranes. NEDC also provided a completely different molecular profile compared to 4-APEBA (Fig. 2D), probably due to the already reported different molecular specificity of the two approaches for imaging electron acceptor molecules,

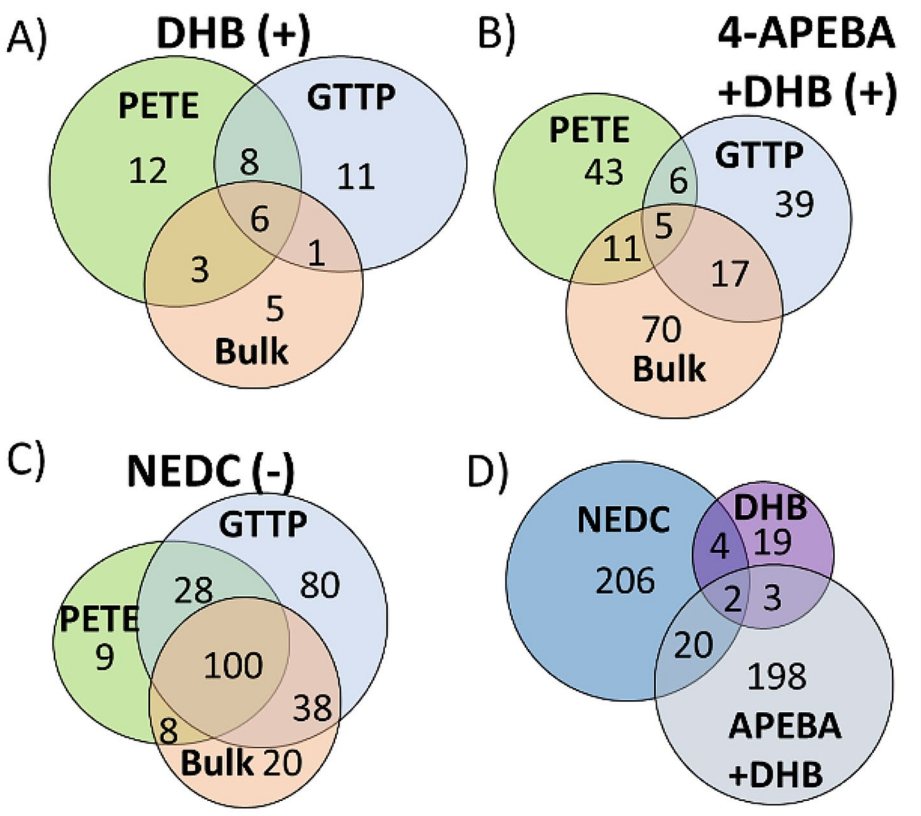

Fig. 2 Number of endogenous annotated MALDI ions by METASPACE using the KEGG database from bulk extract, PETE, or GTTP membranes in different MALDI matrix conditions. Only ions annotated within 20% FDR in at least one condition were considered. **A**) DHB as MALDI matrix **B**) OTCD with 4-APEBA and DHB as MALDI matrix **C**) NEDC as MALDI matrix **D**) overlapped number of annotations in different MALDI matrix conditions. DHB: 2,5-dihydroxybenzoic acid; 4-APEBA: 4-(2-((4-bromophenethyl)dimethylammonio)ethoxy)benzenaminium bromide; NEDC: N-(1-naphthyl) ethylenediamine dihydrochloride; PETE: polyester track etch; GTTP: hydrophilic polycarbonate. The tentative identities of molecules detected in these different conditions are provided in Supplementary Figures (Figure S2-S11)

where NEDC is more specific for aromatic and 4-APEBA OTCD for aliphatic carbonyls [11].

Notably, many ions not detected in the bulk extracts were detected and tentatively annotated on the imprinted membranes, especially using the 4-APEBA workflow. For example, there were 43 such molecules detected from PETE and 39 others detected from GTTP, Fig. 2B. Those ions were almost exclusively present in distinct hot spots, counting less than 0.05% of the entire analyzed area (clusters of ~15–20 pixels out of ~42,000 pixels total), Fig. 3. Their absence in bulk extracts probably results from their dilution below the limit of detection in these bulk measurements, illustrating the necessity for highly sensitive imaging approaches to capture localized biological activities occurring in the rhizosphere. The example is illustrated in Fig. 3, showing hot spots of oxamic acid, a rhizobium natural product that has a role analog to pyruvate [16]. A similar observation occurred when NEDC was used as a matrix, especially when using the GTTP membrane, where we could localize 80 low-abundance and discretely distributed compounds not detected from bulk extracts. We elaborate on some of those molecules and their origin later in the manuscript.

An overview of the tentative identities of molecules detected with different approaches is summarized in the Supplementary Figures (Figure S2-S11). Using 4-APEBA, we detected ions that putatively correspond to hydroxy pyruvate (intermediate in serine biosynthesis) [17], glyoxalate (center molecule for the synthesis of carbohydrates in plants and microbes) [18], indole-3-acetate (phytohormone) [19], and fatty acids from both membranes. Meanwhile, components of the Krebs cycle [20], such as fumaric acid and pyruvate, and amino acids proline and glutamine were only detected from GTTP, whereas shikimate (central metabolite in the microbial and plant pathway for folate and aromatic amino acid synthesis) [21] and hydroperoxy acids (common constituents of microbial and plant lipids) [22] were only detected from PETE when OTCD was used (Figure S2-S4). Even though DHB without derivatization yields relatively poor molecular coverage (Fig. 2A and D), using this MALDI matrix alone, we can detect ions corresponding to biological amines [23] (e.g., taurine, carnitine, valine, and arginine),

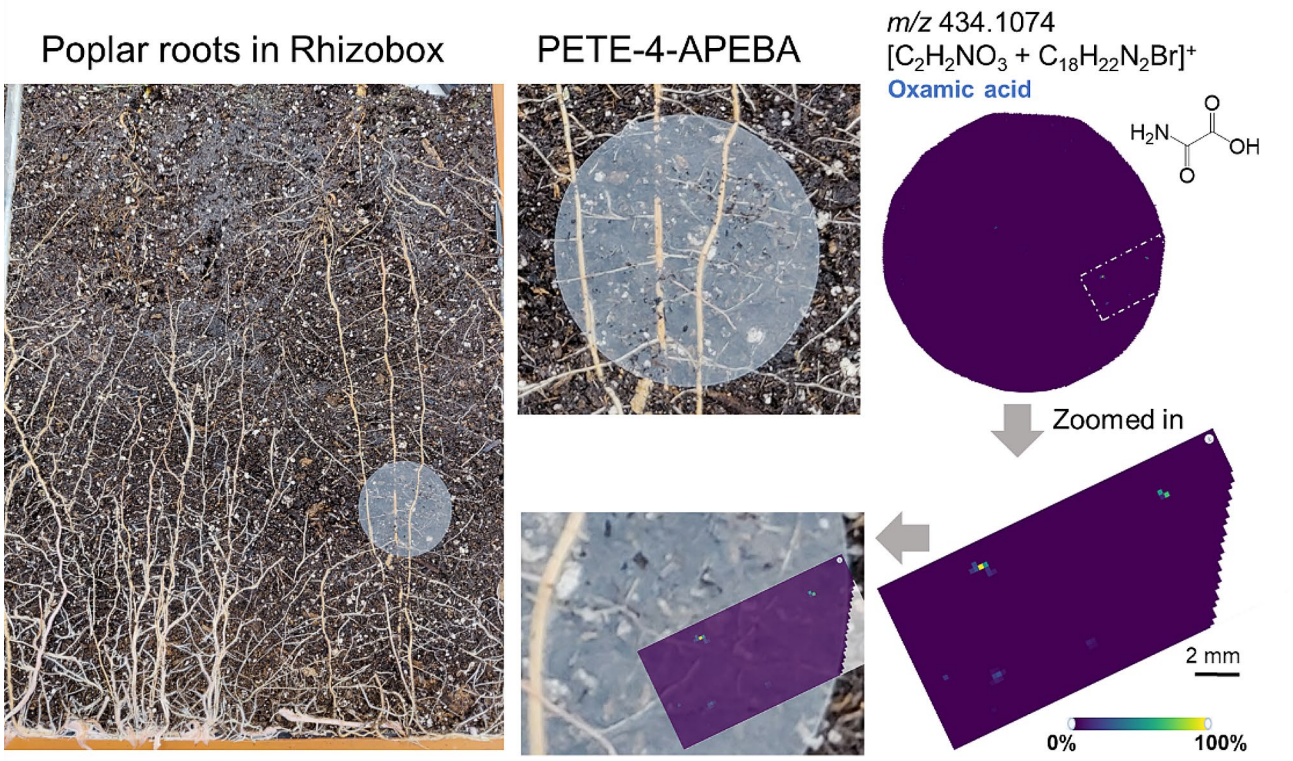

Fig. 3 An example of a MALDI-generated ion tentatively annotated as oxamic acid (*m/z* 434.1074) that is not detected in the bulk extract but was detected only in discrete pixel clusters in the PETE-4-APEBA workflow

Supplementary Figure S5, being they have high proton affinity and ionization efficiency in MALDI. Using NEDC as the MALDI matrix, we additionally visualized the distribution of sugars, sugar alcohols, and many flavonoid compounds and secondary metabolites through both membranes (Supplementary Figure S6-S11). A particular benefit is that using the GTTP-NEDC combination, we visualized the distribution of abscisic acid and salicylic acid, phytohormones that play essential roles in plant growth and development [24, 25].

We observed various distributions of molecules within the rhizosphere (Fig. 4). For example, regarding two phytohormones imaged using the GTTP-NEDC workflow, salicylic acid distribution follows traces of a complex root network. In contrast, abscisic acid has increased concentration only in one microzone in the rhizosphere (Fig. 4A) near the root. Figure 4B shows how octadecanoic acid distribution colocalizes with the roots while hexadecenoic acid is abundant in soil aggregates. This spatial detection of fatty acids illustrates that our RhizoMAP methods enable tracking fatty acid chemistry and distribution in the soil, which could be a potent tool for investigating microbial phenotypes in different soil zones because fatty acids are signatures of soil microbial biomass [26]. The PETE-NEDC workflow indicates disaccharides diffuse from the roots into the surrounding soil (Fig. 4C). However, the origin of these disaccharides might also be from native mycorrhizae in the soil, as their presence is observed by analyzing rhizobox without the plant. The same workflow allowed us to visualize the hot spot of glutathione, a small thiol molecule that maintains a reduced system state, serving as a stress protectant [27], Fig. 4C. The spatial distribution of all other molecules detected using our workflow is publicly available and can be visualized using the METASPACE link provided in the Availability of data and materials section.

Comparing imprints from rhizobox that did not contain poplar roots with the rhizobox that contained a complex root network, RhizoMAP revealed molecules that have soil origin and those that are produced, transformed, or consumed as a consequence of root growth in the soil, Fig. 5. Herein, "soil with root" refers to the membrane that was placed in the poplar Rhizobox, "soil without root" to the membrane placed in the Rhizobox filled only with the soil, and "blank" to the membrane that was not placed in the Rhizobox and hence has never been in contact with soil and root. We were able to monitor the changes in the metabolite profile of the mycorrhizae soil during root growth, where 50 new annotated ion features were detected when the root was present in the soil, 23 identical features were annotated in both conditions, and 33 features were detected only in the soil without plant (Fig. 5A). For example, galactose metabolism is active in the poplar rhizosphere but not in the mycorrhizae

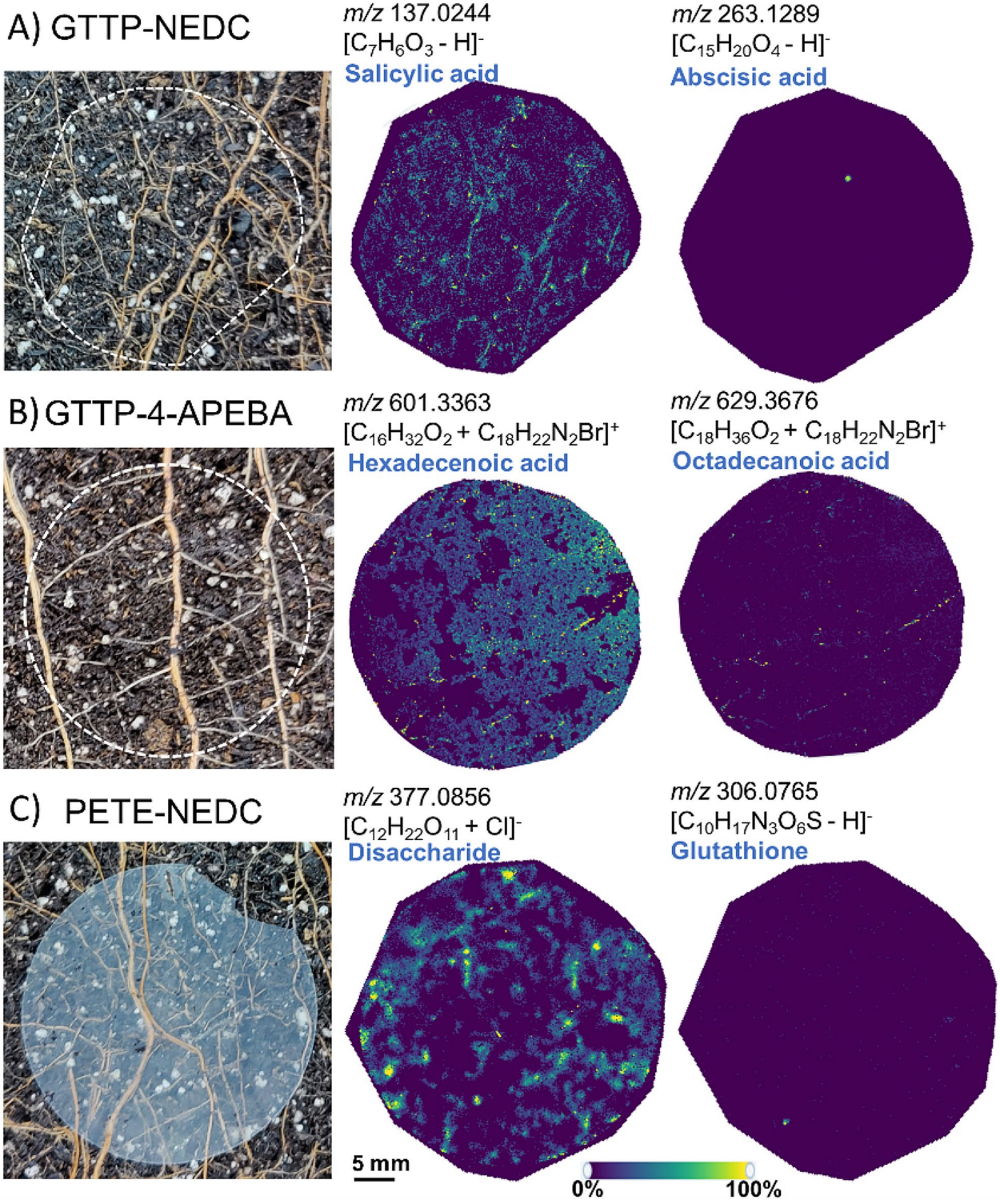

Fig. 4 Example of spatial distributions of organics observed through different membrane-matrix approaches. **A**) GTTP-NEDC: ion images of deprotonated molecules tentatively annotated as salicylic acid (*m/z* 137.0244) and abscisic acid (*m/z* 263.1289, 0.06 ppm error) **B**) GTTP-4-APEBA: ion images of derivatized molecules tentatively annotated as hexadecenoic acid (*m/z* 601.3363) and oxadecanoic acid (*m/z* 629.3676) **C**) PETE-NEDC: ion images of deprotonated molecules tentatively annotated as a disaccharide (*m/z* 377.0856) and glutathione (*m/z* 263.1289)

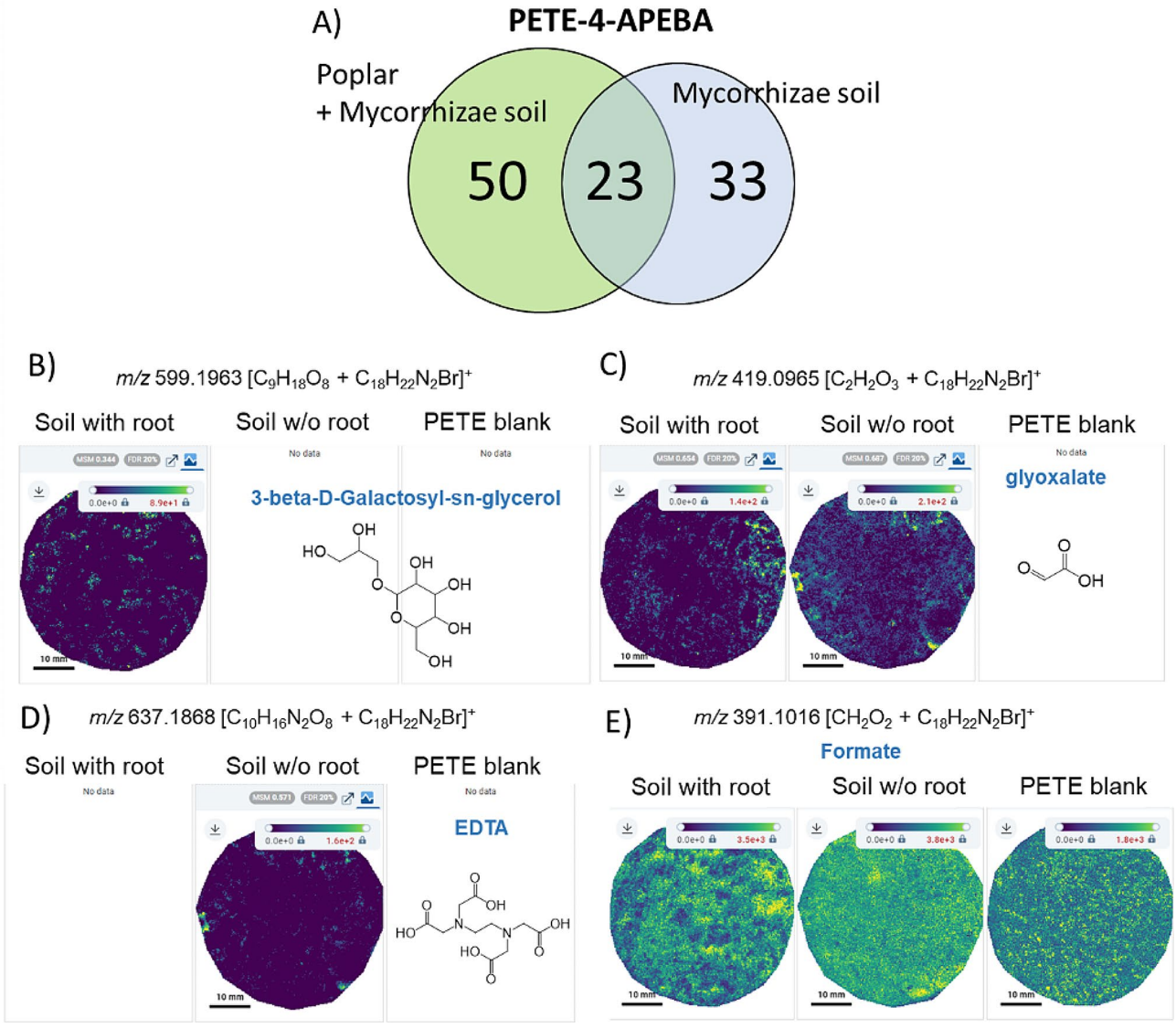

Fig. 5 Differentiation between organics present in the soil and those originated by plant growth. **A**) Number of ion images from controlled mycorrhizae soil (without poplar) and mycorrhizae soil with poplar roots, annotated by the KEGG database in PETE-4-APEBA conditions. **B**) An example of an ion image detected only from Rhizobox with poplar roots (poplar + mycorrhizae soil) with 3-beta-D-galactosyl-sn-glycerol (*m/z* 599.1963) annotated. **C**) An example of an ion image detected from mycorrhizae soil without and with root with glyoxalate (*m/z* 419.0965) annotated. **D**) An example of an ion image detected only in mycorrhizae soil annotated as EDTA (m/z 637.1868). **E**) An example of false positive annotation: an ion image annotated as formic acid (*m/z* 391.1016) is detected in the clean membrane (PETE blank). Note that because METASPACE was used to compare datasets, ion images of molecules not detected in the specific treatment were not included as they were not annotated and hence displayed in METASPACE

soil (Fig. 5B), whereas the glyoxalate cycle occurs in the mycorrhizae soil, even without the plant (Fig. 5C).

Interestingly, ethylenediaminetetraacetic acid (EDTA) is one of the molecules detected only in the soil without poplar (Fig. 5D). This chelating molecule which serves to solubilize metals and make them more accessible to plants [28] was a component of the fertilizer we used, so it might be that its concentration decreased below the detection limit as the plant consumed chelated metals during growth [29]. Moreover, analyzing a clean membrane (PETE blank) that has never been in contact with the soil or the root allowed us to eliminate false positives (e.g., background annotations). For example, we can see a homogeneously distributed signal from PETE blank annotated as formic acid; therefore, it does not have rhizosphere origin (Fig. 4E). Supplementary Figures S12-S14 provide a complete list of molecules that are associated with mycorrhizae soil with or without poplar.

Ultimately, we demonstrated the power of our RhizoMAP protocol in imaging gradients of root exudation

and organics throughout the entire rhizosphere depth and root growth zones, Fig. 6. We placed GTTP membranes on areas along the root growth and analyzed them using the 4-APEBA workflow. We observed various spatial patterns of molecular distributions, some depicted in Fig. 6. For example, we detected an ion at *m/z* 863.4204 that colocalizes uniformly with the entire root tissue and whose molecular formula suggests it might be cucurbitacin or another mass isomer of this highly oxidized tetracyclic triterpenoid. Those molecules are widely distributed in the plant kingdom and act as heterologous chemical pheromones that protect plants from external biological insults [30], and it seems, based on our imaging data, that they remain highly associated with the root surface and don't diffuse in the surrounding rhizosphere. On the contrary, pyruvate, glyoxalate, methylglyoxal, and glyoxal share a distribution pattern where the highest abundance is associated with the root traces, suggesting possible exudation of these molecules along the entire root length into the soil pores. Creating a methodology such as RhizoMAP that enables insight into the relative abundance of these oxygenated short aldehydes (methylglyoxal and glyoxal) in the rhizosphere is of the utmost importance as those molecules are produced in plants as a by-product of many metabolic reactions and are identified as emerging signaling molecules in plant abiotic stress responses [31]. The third example of observed spatial distribution is the localization of oxoproline, a plant intermediate in the glutathione cycle [32]. This metabolite was observed only in the root base tissue and without exudation (diffusion) in the surrounding soil. Interestingly, this aligns well with a recent report that suggests that oxoproline was only detected in root exudates from poplars grown in sterilized but not soil populated by microbes [33] Supplementary Table 1 provides the complete list of metabolites detected in this experiment, together with their localization in the rhizosphere.

Discussion

The RhizoMAP platform described in this manuscript enables insight into spatial distribution of several hundred metabolites and small organics in the rhizosphere, their potential biological origin, hot spots of metabolic activities, exudation dynamics, and microscale molecular gradients from root base to root tip. The foundation of the RhizoMAP is MALDI-MSI of the rhizosphere imprints, relying on the specific membranes for efficient molecular transfer and compatibility with MALDI process, and therefore several factors were considered for reliable results.

One of the main prerequisites for successful and reliable MALDI-MSI is the high and stable total ion current during the entire imaging run without areas on the sample that will cause a significant drop. This ensures

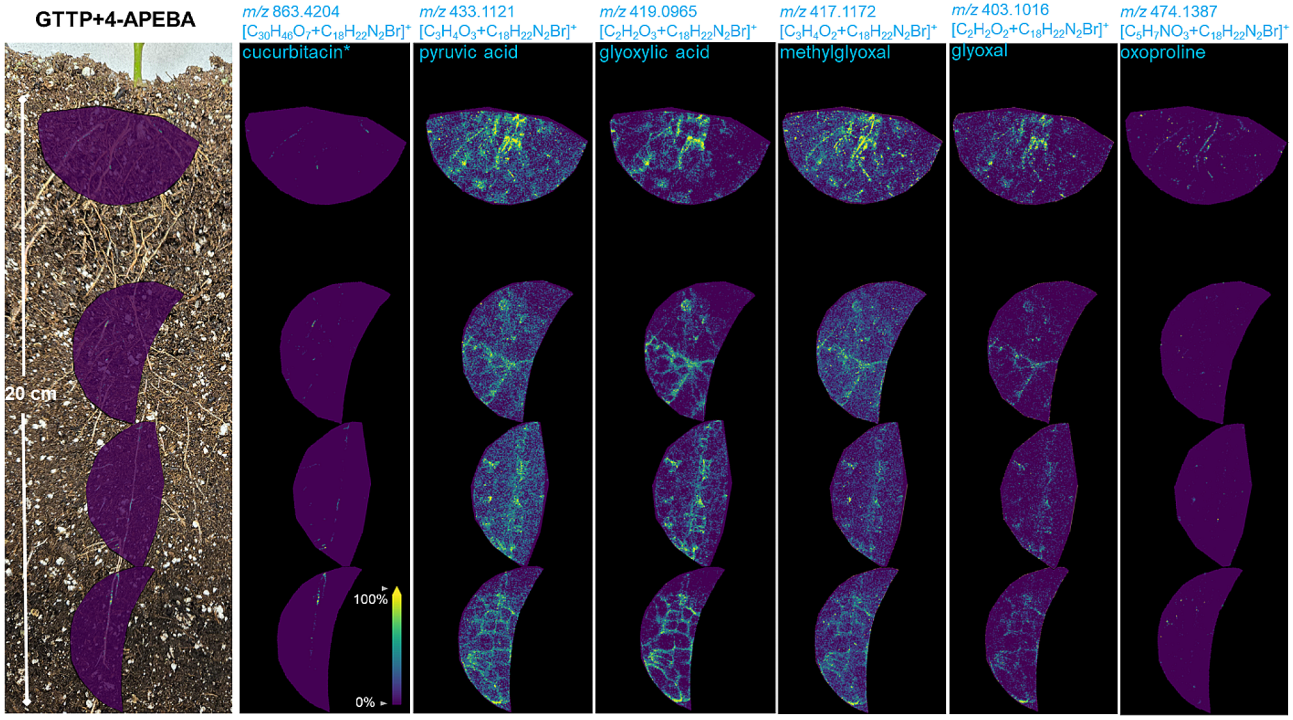

Fig. 6 Spatial distribution of exemplary rhizosphere organics throughout the root length and associated rhizosphere. Highlighted annotations consist of cucurbitacin* (*m/z* 863.4204), pyruvic acid (*m/z* 433.1121), glyoxylic acid (*m/z* 419.0965), methylglyoxal (*m/z* 417.1172), glyoxal (*m/z* 403.1016), and oxoproline (*m/z* 474.1387). Four GTTP membranes were placed at different root zones from the root base to the root tip and, after blotting, were analyzed using the 4-APEBA OTCD workflow. An asterisk (*) indicates the potential of isomers being annotated alongside the named compound

high sensitivity of analysis and that different intensities of MS signal in different areas of the sample reflect the relative abundance of the molecule in the sampling areas. The unstable total ion current is particularly emphasized in imprinting analyses where membrane can add a significant electrical insulation barrier for transferring MALDI-generated ions through the mass spectrometer. This is the reason why the membranes' thicknesses in RhizoMAP significantly enhanced sensitivity and the number of annotated species compared to our pioneering work where PVDF membranes were used [11]. More specifically, the GTTP and PETE membranes we used in the current study were 17 µm and 12 µm thick, respectively, which puts them in the ideal range for MALDI-MSI analysis [34].

On the contrary, PVDF membranes used in our primer work were ~120 µm thick, causing a significant drop in the total ion current in the central zones of the large membranes and, even more, an inability to perform negative ion mode analysis [11]. This inability is a significant limitation as most plant-derived metabolites are readily detected in negative ionization mode due to their acidic (electron acceptor) chemistry, and as such, analysis in positive ionization mode can hinder the presence of many essential phytocompounds. This selectivity is also observed in our results, where molecular coverage in the positive ionization mode using DHB is relatively poor compared to the negative ionization mode analysis using NEDC as the MALDI matrix. Recently, our group established an OTCD workflow using 4-APEBA that converts acidic carbonyls (i.e., ketones, aldehydes, and carboxylic acids) to permanently positive charged derivatives, allowing them to be spatially profiled in the positive ionization mode from biological samples [15]. We used this OTCD approach to our advantage in the rhizosphere imprint imaging to expand the molecular coverage in RhizoMAP. Obviously, membrane chemistry and the choice of the MALDI matrix play a huge role in the obtained molecular profile, and it is the reason why RhizoMAP uses both PETE and GTTP membranes with 4-APEBA, DHB, and NEDC conditions to cover a vast repertoire of molecules and metabolic pathways. As such it covers molecules involved in the various rhizosphere processes: from very abundant sugars to low abundant phytohormones and highly specified secondary metabolites. Note that the number of annotated molecules discussed throughout the manuscript is based on the annotations from the KEGG database, which includes many plant molecules. However, we expect this number to be higher as many secondary metabolites from mycorrhizae and soil organic matter might not be captured in the KEGG database, so including experimentally generated databases, plant-specific databases, or targeted searches could reveal even more interesting findings.

One open question on the RhizoMAP workflow is, since roots are not entirely exposed to the surface (with parts buried below the outermost soil layer), the efficiency of the contact between the membrane and root-soil interface in the rhizobox. However, the GTTP and PETE membranes used in this study were highly flexible and adaptable to the topography of the rhizosphere surface. Additionally, pressure and better contact are ensured by tightening the glass panels of the rhizobox, but in practice, efficient contact cannot be fully controlled. This can also explain why some molecules were observed as sparse hot spots, where the contact and the transfer of molecules through passive imprinting were possibly the most efficient. Nonetheless, the ability to detect hundreds of low-abundance molecules that were not observed using the traditional extraction approach, makes RhizoMAP the most sensitive method for revealing hot spots of metabolic activity in the rhizosphere without destructive sampling.

Conclusion

The RhizoMAP approach presented in this manuscript is an untargeted, nondestructive, robust, versatile, and readily adaptable methodology that enables a deep metabolic coverage of rhizosphere biochemistry on the micrometer scales. We demonstrated how a wide range of molecules could be spatially profiled from the rhizosphere composed of poplar roots and associated soil organic matter and how RhizoMAP can be used to differentiate the biological origin of rhizosphere compounds, track the degree of diffusion of root exudates in the surrounding soil and monitor gradients of surface root metabolites along the root. As such, we envision that RhizoMAP, in its current form, will find new and attractive applications in tracking molecular perturbations, relocation, and transformation for a better understanding of various underground questions related to plant health, nutrient cycling, disease management, environmental impact, and agricultural productivity. Experiments outlined within the RhizoMAP protocol will also further drive the understanding of metabolic hotspots, endophyte recruitment, and microbe-soil-plant interactions, where diverse biotic and abiotic stressors can be routinely applied within controlled greenhouse environments.

Abbreviations

4 APEBA	4-2-4-bromophenethyl)dimethylammonio)ethoxy) benzenaminium bromide
DESI	Desorption electrospray ionization
DHB	2,5-Dihydroxybenzoic acid
EDC	1-ethyl-3-(3-dimethylaminopropyl)carbodiimide
EDTA	Ethylenediaminetetraacetic acid
FTICR	Fourier transform ion cyclotron resonance
GTTP	Hydrophilic polycarbonate
MALDI	Matrix-assisted laser desorption/ionization
MeOH	Methanol
MRMS	Magnetic resonance mass spectrometry

MSI	Mass spectrometry imaging
NEDC	N-(1-Naphthyl) Ethylenediamine dihydrochloride
OTCD	On-target chemical derivatization
PETE	Polyester track etch
PVDF	Polyvinylidene fluoride

Supplementary Information

The online version contains supplementary material available at https://doi.org/10.1186/s13007-024-01249-5.

Supplementary Material 1

Supplementary Material 2

Supplementary Material 3

Acknowledgements
Not applicable.

Author contributions
D.V. obtained funding and administered the project. D.V. conceptualized the project and performed MALDI-MSI analyses. T.W, V.K, and A.A conducted plant experiments. T.W designed and constructed rhizoboxes. K.Z and C.A helped in the MALDI imaging data interpretation. D.V wrote the initial manuscript draft. A.A, K.Z, and C.A reviewed and edited the manuscript. All authors have read and agreed to the published version of the manuscript.

Funding
This research was performed on a project award https://doi.org/10.46936/intm.proj.2023.60889/60008968(D.V.) from the Environmental Molecular Sciences Laboratory, a DOE Office of Science User Facility sponsored by the Biological and Environmental Research program under Contract No. DE-AC05-76RL01830.

Data availability
Data is provided within the manuscript or supplementary information files.

Declarations

Ethics approval and consent to participate
Not applicable.

Consent for publication
Not applicable.

Competing interests
The authors declare no competing interests.

Author details
[1]Environmental Molecular Sciences Laboratory, Pacific Northwest National Laboratory, Richland, WA 99354, USA

Received: 11 June 2024 / Accepted: 28 July 2024
Published online: 02 August 2024

References

1. Védère C, Gonod LV, Nunan N, Chenu C. Opportunities and limits in imaging microorganisms and their activities in soil microhabitats. Soil Biol Biochem. 2022;174.
2. Ma WM, Tang SH, Dengzeng Z, Zhang D, Zhang T, Ma XL. Root exudates contribute to belowground ecosystem hotspots: a review. Front Microbiol. 2022;13.
3. Ahkami AH, Qafoku O, Roose T, Mou QB, Lu Y, Cardon ZG et al. Emerging sensing, imaging, and computational technologies to scale nano-to macroscale rhizosphere dynamics - review and research perspectives. Soil Biol Biochem. 2024;189.
4. Lippold E, Schlüter S, Mueller CW, Höschen C, Harrington G, Kilian R, et al. Correlative imaging of the Rhizosphere-A Multimethod Workflow for targeted mapping of Chemical gradient (57, Pg 1538, 2023). Environ Sci Technol. 2023;57(45):17660.
5. Koop-Jakobsen K, Mueller P, Meier RJ, Liebsch G, Jensen K. Plant-sediment interactions in Salt marshes - an Optode Imaging Study of O, pH, and CO gradients in the Rhizosphere. Front Plant Sci. 2018;9.
6. Zhang XC, Bilyera N, Fan LC, Duddek P, Ahmed MA, Carminati A, et al. The spatial distribution of rhizosphere microbial activities under drought: water availability is more important than root-hair-controlled exudation. New Phytol. 2023;237(3):780–92.
7. Lin VS, Rosnow JJ, McGrady MY, Smercina DN, Nuñez JR, Renslow RS et al. Non-destructive spatial analysis of phosphatase activity and total protein distribution in the rhizosphere using a root blotting method. Soil Biol Biochem. 2020;146.
8. Velickovic D, Anderton CR. Mass spectrometry imaging: towards mapping the elemental and molecular composition of the rhizosphere. Rhizosphere-Neth. 2017;3:254–8.
9. Lohse M, Haag R, Lippold E, Vetterlein D, Reemtsma T, Lechtenfeld OJ. Direct Imaging of Plant Metabolites in the Rhizosphere using laser desorption ionization Ultra-high Resolution Mass Spectrometry. Front Plant Sci. 2021;12.
10. Aufrecht J, Khalid M, Walton CL, Tate K, Cahill JF, Retterer ST. Hotspots of root-exuded amino acids are created within a rhizosphere-on-a-chip. Lab Chip. 2022;22(5):954–63.
11. Velickovic D, Lin VS, Rivas A, Anderton CR, Moran JJ. An approach for broad molecular imaging of the root-soil interface via indirect matrix-assisted laser desorption/ionization mass spectrometry. Soil Biol Biochem. 2020;146.
12. Liu C, Ding TX, van der Ent A, Liu C, Morel JL, Sirguey C, et al. A novel method for in situ imaging of root exudates and labile elements reveals phosphorus deficiency-induced mobilization of rare earth elements in the rhizosphere of. Plant Soil. 2024;495(1–2):13–26.
13. Tfaily MM, Chu RK, Toyoda J, Tolic N, Robinson EW, Pasa-Tolic L, et al. Sequential extraction protocol for organic matter from soils and sediments using high resolution mass spectrometry. Anal Chim Acta. 2017;972:54–61.
14. Zemaitis KJ, Lin VS, Ahkami AH, Winkler TE, Anderton CR, Velickovic D. Expanded Coverage of Phytocompounds by Mass Spectrometry Imaging using On-Tissue chemical derivatization by 4-APEBA. Anal Chem. 2023.
15. Velickovic D, Zemaitis KJ, Bhattacharjee A, Anderton CR. Mass spectrometry imaging of natural carbonyl products directly from agar-based microbial interactions using 4-APEBA derivatization. Msystems. 2024;9(1).
16. Marlier JF, Cleland WW, Zeczycki TN. Oxamate is an alternative substrate for pyruvate carboxylase from. Biochemistry-Us. 2013;52(17):2888–94.
17. Timm S, Florian A, Jahnke K, Nunes-Nesi A, Fernie AR, Bauwe H. The hydroxypyruvate-reducing system in Arabidopsis: multiple enzymes for the same end. Plant Physiol. 2011;155(2):694–705.
18. De Bellis L, Luvisi A, Alpi A, Aconitase. To be or not to be inside plant glyoxysomes, that is the question. Biology-Basel. 2020;9(7).
19. Duca D, Lorv J, Patten CL, Rose D, Glick BR. Indole-3-acetic acid in plant-microbe interactions. Anton Leeuw Int J G. 2014;106(1):85–125.
20. Zhang YJ, Fernie AR. On the role of the tricarboxylic acid cycle in plant productivity. J Integr Plant Biol. 2018;60(12):1199–216.
21. Tzin V, Galili G. New insights into the Shikimate and aromatic amino acids biosynthesis pathways in plants. Mol Plant. 2010;3(6):956–72.
22. Griffiths G, Leverentz M, Silkowski H, Gill N, Sánchez-Serrano JJ. Lipid hydroperoxide levels in plant tissues. J Exp Bot. 2000;51(349):1363–70.
23. Bouchereau A, Guénot P, Lather F. Analysis of amines in plant materials. J Chromatogr B. 2000;747(1–2):49–67.
24. Chen K, Li GJ, Bressan RA, Song CP, Zhu JK, Zhao Y. Abscisic acid dynamics, signaling, and functions in plants. J Integr Plant Biol. 2020;62(1):25–54.
25. Klessig DF, Tian MY, Choi HW. Multiple targets of salicylic acid and its derivatives in plants and animals. Front Immunol. 2016;7.
26. Joergensen RG. Phospholipid fatty acids in soil-drawbacks and future prospects. Biol Fert Soils. 2022;58(1):1–6.
27. Hasanuzzaman M, Nahar K, Anee TI, Fujita M. Glutathione in plants: biosynthesis and physiological role in environmental stress tolerance. Physiol Mol Biol Pla. 2017;23(2):249–68.
28. Liphadzi MS, Kirkham MB. Availability and plant uptake of heavy metals in EDTA-assisted phytoremediation of soil and composted biosolids. S Afr J Bot. 2006;72(3):391–7.
29. Chen YH, Li XD, Shen ZG. Leaching and uptake of heavy metals by ten different species of plants during an EDTA-assisted phytoextraction process. Chemosphere. 2004;57(3):187–96.

30. Alghasham AA. Cucurbitacins - a promising target for cancer therapy. Int J Health Sci (Qassim). 2013;7(1):77–89.
31. Hoque TS, Hossain MA, Mostofa MG, Burritt DJ, Fujita M, Tran LSP. Methylglyoxal: an Emerging Signaling Molecule in Plant Abiotic stress responses and tolerance. Front Plant Sci. 2016;7.
32. Mazelis M, Pratt HM. In vivo conversion of 5-oxoproline to glutamate by higher plants. Plant Physiol. 1976;57(1):85–7.
33. Fracchia F, Guinet F, Engle NL, Tschaplinski TJ, Veneault-Fourrey C, Deveau A. Microbe tree metabolite interactions in the soil - phyllosphere continuum of poplar tree: when microbes rewire poplar root exudate and metabolome. bioRxiv. 2024.
34. Wang XF, Zhang L, Xiang YH, Ye NS, Liu KH. Systematic study of tissue section thickness for MALDI MS profiling and imaging. Analyst. 2023;148(4):888–97.

Publisher's Note